Measurement of the Static Structure Factor in a Paraxial Fluid of Light Using Bragg-like Spectroscopy

Clara Piekarski, Wei Liu, Jeff Steinhauer, Elisabeth Giacobino, Alberto Bramati, Quentin Glorieux

Measurement of the Static Structure Factor in a Paraxial Fluid of Light Using Bragg-like Spectroscopy

Clara Piekarski,[1] Wei Liu,[1] Jeff Steinhauer,[1,2] Elisabeth Giacobino,[1] Alberto Bramati,[1] and Quentin Glorieux[1,*]
[1]Laboratoire Kastler Brossel, Sorbonne Universit, CNRS, ENS-PSL Research University, Collège de France, Paris 75005, France
[2]Department of Physics, TechnionIsrael Institute of Technology, Technion City, Haifa 32000, Israel

(Received 17 December 2020; accepted 11 June 2021; published 7 July 2021)

We implement Bragg-like spectroscopy in a paraxial fluid of light by imprinting analogues of short Bragg pulses on the photon fluid using wavefront shaping with a spatial light modulator. We report a measurement of the static structure factor, $S(k)$, and we find a quantitative agreement with the prediction of the Feynman relation revealing indirectly the presence of pair-correlated particles in the fluid. Finally, we improve the resolution over previous methods and obtain the dispersion relation including a linear phononic regime for weakly interacting photons and low sound velocity.

DOI: 10.1103/PhysRevLett.127.023401

Fluids of light in the paraxial configuration have emerged as an original approach to study degenerate Bose gases [1]. Several important results have recently established this platform as a potential analogue quantum simulator, including the demonstrations of superfluidity of light [2–4], the observation of the Berezinskii-Kosterlitz-Thouless transition [5], shockwaves [6–8] and precondensation [9], the evidence of photon droplets [10], and the creation of analogue rotating black hole geometries [11,12]. Paraxial fluids of light rely on the direct mathematical analogy that can be drawn between the Gross-Pitaevskii equation describing the mean field evolution of a Bose-Einstein condensate (BEC) and the nonlinear Schrödinger equation describing the propagation of light within a $\chi^{(3)}$ nonlinear medium [1,13,14]. The growing interest about this platform comes from the various advantages that make paraxial fluids of light a complementary system to an atomic BEC. First, optical detection techniques are highly sensitive (single-photon counting, homodyne detection) and allow for measuring with high precision the density distribution in position and momentum space as well as the phase. Second, since there is no gravity force acting on a photon fluid, there is no need for a trapping potential and homogeneous density can be easily achieved. Moreover, an external control potential can be applied either during the entire evolution [3,15], or only for a short period of time as in this work.

An essential characterization tool for an atomic BEC is coherent Bragg spectroscopy [16]. The original implementation was based on two-photon Bragg scattering and allowed for an accurate measurement of the momentum distribution, which was significantly narrower than that observed by time of flight [17]. For an atomic BEC, it was realized very early that this technique would also allow for measuring both the dispersion relation [18], which describes how each frequency component of a wave packet evolves, and the dynamic structure factor, which is the Fourier transform of the density correlation function [19] and is essential to the description of many-body systems [20,21].

Several variants of this method have been developed for exciton polaritons [22] and for atomic BECs, including momentum-resolved spectroscopy [23], multibranch spectroscopy [24], and tomographic imaging [25]. Most of these techniques rely on measuring the energy of the condensate's linear excitations known as the Bogoliubov quasiparticles. While, the dispersion relation has been recently obtained by measuring the group velocity of two counterpropagating wave packets [2], a measurement of the static structure factor, that characterizes the density-density correlations of the elementary excitations, has not yet been reported for a fluid of light.

In this Letter, we implement an optical analogue of Bragg spectroscopy to measure the static structure factor in a paraxial fluid of light. We show that short Bragg pulses used for the phase imprinting technique in an atomic BEC [26] can be achieved in a photon fluid by using wave front shaping with a spatial light modulator. We found that the static structure factor is significantly reduced at long wavelength, compared to that of free particles, revealing indirectly the presence of nontrivial pair correlations in a paraxial fluid of light [18]. In addition, we show that our method allows for an improvement of the resolution for dispersion measurements.

This Letter is organized as follows. We first introduce the formalism of a paraxial fluid of light and the short Bragg pulse technique which inspired our approach. We describe numerically and experimentally the optical implementation of Bragg spectroscopy. We then present a measurement of the static structure factor in agreement with the Feynman

relation for a homogeneous Bose gas [20,27]. Finally, we measure the dispersion relation and evaluate the maximum resolution of our technique.

In a third-order nonlinear Kerr medium, the evolution of the electric field is given by the nonlinear Schrödinger equation (NLSE), written within the paraxial and slowly-varying-envelope approximation as

$$i\frac{\partial E}{\partial z} = \left(-\frac{1}{2k_0}\nabla_\perp^2 - k_0 n_2|E|^2 + i\frac{\alpha}{2}\right)E, \tag{1}$$

where k_0 is the wave vector, α is the linear absorption coefficient, and n_2 is the nonlinear index. The subscript $\perp$ refers to the transverse (x, y) plane. We define $\Delta n = n_2|E|^2$ as the nonlinear refractive index.

What is remarkable about this equation is that it is similar to the Gross-Pitaevskii equation (GPE), which describes the evolution of the wave function Ψ of a weakly interacting Bose-Einstein condensate:

$$i\hbar\frac{\partial \Psi(\mathbf{r}, t)}{\partial t} = \left(-\frac{\hbar^2}{2m}\nabla^2 + \mathcal{V}(\mathbf{r}) + g|\Psi(\mathbf{r}, t)|^2\right)\Psi(\mathbf{r}, t), \tag{2}$$

where $\mathcal{V}$ is the trapping potential, m is the bosonic mass, and g is the interaction parameter, which is positive for a stable condensate.

To map the NLSE onto the GPE, we define an effective time $\tau = z/c$. This space-time mapping means that each transverse plane inside the nonlinear medium is formally analogous to a 2D Bose gas of photons after the corresponding effective time of evolution τ. Since the z dimension acts as an effective time dimension, this configuration is referred as 2D + 1 geometry.

The comparison between the NLSE and the GPE yields expressions for the effective photon mass $\bar{m} = \hbar k_0/c$ and for the interaction term $\bar{g} = -\hbar c k_0 n_2$. In our case, the stability condition $\bar{g} > 0$ corresponds to $\Delta n < 0$ (i.e., self-defocusing regime). One can notice that there is no trapping potential term in Eq. (1), as fluids of light do not need to be held in a trap. The term $i(\alpha/2)E$ in Eq. (1) corresponds to absorption and is therefore not present in Eq. (2). For $\alpha \leq 13\ \mathrm{cm}^{-1}$ (transmission larger than 60%), we verified numerically that absorption can be neglected since it does not modify significantly the behavior of our system.

In a weakly interacting BEC the excitation spectrum is given by the Bogoliubov dispersion relation $\Omega_B(\mathbf{k}_x)$ [28], which can be rewritten for a photon fluid as [1]

$$\Omega_B(\mathbf{k}_x) = \sqrt{\left(\frac{k_x^2}{2k_0}\right)^2 + k_x^2\Delta n}, \tag{3}$$

where k_x is the wave number in the transverse direction. Within space-time mapping, Ω_B has units of an inverse length. Equation (3) shows two regimes of dispersion, with a transition that occurs around $k_x = k_0\sqrt{|\Delta n|} = 1/\xi$ with ξ as the healing length. For $k_x\xi < 1$, the dispersion is linear and Bogoliubov excitations present a phononlike behavior: $\Omega_B \approx k_x\sqrt{\Delta n}$. For $k_x\xi > 1$, the dispersion becomes quadratic: $\Omega_B \approx k_x^2/2k_0$. In this regime, excitations have the same dispersion as free massive particles.

Bragg spectroscopy in an atomic BEC relies on counting the number of scattered atoms as a function of the frequency difference between two Bragg beams. A variant of this configuration has been presented in [26] and relies on short Bragg pulses at two symmetrically tilted angles to imprint a phase pattern on a BEC at time $t = 0$. The short pulse results in a broad frequency perturbation, which ensures the creation of counterpropagating phonons at wave vectors $+k_x$ and $-k_x$, corresponding to a standing wave in the BEC density. The density perturbation after a time t, defined as $\delta n(t) = |\psi(t)|^2 - |\psi(t = 0)|^2$, has a spectrum given by the Bogoliubov dispersion relation. In [26], the authors measured the spatial Fourier transform $\rho_k(t)$ of $\delta n(t)$, and they extracted the Bogoliubov pulsation from the zero-crossings (in time) of $\rho_k(t)$.

To design an analogue technique for paraxial fluids of light, we made two major modifications. First, we only have access to one value of t which is given, in our analogy, by the length of the nonlinear medium. Therefore, instead of probing the density perturbation as a function of time, we probe it as a function of k_x at fixed effective time $\tau = L/c$. Using only a measurement at the fixed effective time, we show in the following that we can obtain the dispersion relation from the minima of δn, and the zero temperature static structure factor from the maxima of δn.

The second important change concerns the creation of the phase modulation. Rather than applying a sinusoidal potential, we can directly imprint a phase on the laser beam with a spatial light modulator (SLM) and image it on the input plane of the medium. By imposing a sinusoidal phase pattern on the SLM with a given wavelength and a given depth, we create two left and right propagating phonons (see Fig. 1) with the exact same characteristics as in short Bragg pulse spectroscopy. This is in fact a general strength of paraxial fluids of light, since any phase modulation (analogous to any short external potential) can be applied on the initial state of our system.

The propagation of the density perturbation $\delta n(z)$, is then calculated for a 1D + 1 fluid of light with sinusoidal phase modulation at k_x. Using the Bogoliubov approach, this configuration can be understood as a linear superposition of plane waves counterpropagating in the transverse plane with opposite wave vectors $+k_x$ and $-k_x$ and oscillating in z at the angular frequency $\Omega_B(k_x)$ as represented in Figs. 2(a) and 2(b). Since the incoming phase pattern is periodic, Fig. 2(b) is an example of the nonlinear Talbot effect [29,30]. However, no fractal structures are observed as the modulation used here is a smooth sinusoidal grating [31].

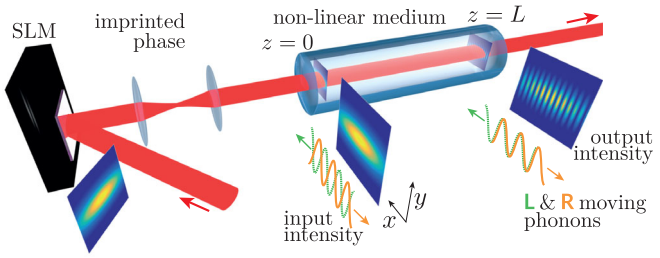

FIG. 1. Principle of the experiment and simplified setup. A 780 nm laser beam is elongated in the x direction and impinges on a spatial light modulator (SLM). The SLM displays a vertical grating, which imprints a sinusoidal phase modulation of wave vector k_x. The SLM plane is imaged at the input of the 6.7 cm rubidium vapor cell. This phase modulation creates two counterpropagating left (L) and right (R) phonons at $+k_x$ and $-k_x$ represented in green and orange. Initially in phase opposition (constant input density), the phonons constructively interfere after some effective time $\tau = z/c$, giving a maximum of density contrast. The output plane of the nonlinear medium (a rubidium vapor cell) is imaged on a camera to study the fringe contrast at $z = L$.

Interference fringes along the transverse axis x with wave vector k_x and fringes along the propagation axis z (i.e., effective time τ) with frequency $\Omega_B(k_x)$ can be observed. Figure 2(a) presents the simulated pattern in the noninteracting case while Fig. 2(b) includes repulsive interactions given by $|\Delta n| = 2.1 \times 10^{-5}$. The reduction of the fringe period along z reflects the difference between the free-particle dispersion (a) and the Bogoliubov dispersion (b) due to the interaction energy. As mentioned earlier, we cannot directly observe the time evolution in our paraxial fluid of light, since we can only see it at the effective times $\tau = 0$ and $\tau = L/c$. However, we can measure the density contrast at the end of the medium ($z = L$) as a function of k_x, defined by $C = (n_{\max} - n_{\min})/(n_{\max} + n_{\min})$

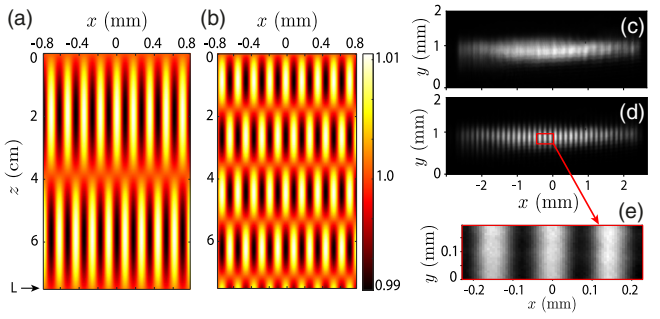

FIG. 2. (a),(b) The simulated density modulation for medium of 7.5 cm and a transverse wave vector of $k_x = 36.0\ \mathrm{mm}^{-1}$, with $\Delta n = 0$ (a) and $\Delta n = 2.1 \times 10^{-5}$ (b). (c),(d) Experimental images of the density obtained respectively for $k_x = 27.8\ \mathrm{mm}^{-1}$ (minimum of contrast) and $k_x = 43.2\ \mathrm{mm}^{-1}$ (maximum of contrast) in the noninteracting case ($\Delta n = 0$). These images are taken with a large modulation depth for illustration. (e) An inset of (d).

and extract the static structure factor $S(k_x)$ from this measurement.

The structure factor is the spatial noise spectrum (normalized to 1 for a coherent state). It is defined by

$$S(k_x) = \frac{\langle \rho_{k_x}^2 \rangle - \langle \rho_{k_x} \rangle^2}{N}, \tag{4}$$

where ρ_{k_x} is the spatial Fourier transform of δn and N the total number of photons. It can be shown [26] that the interference of counterpropagating phonons of wave vector $\pm k_x$ produces a density modulation

$$\delta n(z) = US(k_x) \cos(\mathbf{k}.\mathbf{r}) \sin(\Omega_B z), \tag{5}$$

where U is a constant quantifying the excitation strength. Using the definition of the contrast C in the transverse plan ($\mathbf{r}$) given above, we obtain

$$C(k_x) = |US(k_x) \sin(\Omega_B z)|. \tag{6}$$

In Eq. (6), we can isolate $US(k_x)$ using the contrast maximum values. In order to remove the U dependence, we measure $US(k_x)$ for the noninteracting case. In this regime it is known that $S(k_x)$ is equal to 1 at all k_x since the beam here is a spatially coherent state [28] and therefore U is equal to the contrast maxima.

To implement this procedure experimentally, we use a 780 nm diode laser for which we can finely adjust the frequency detuning Δ with respect to the $F = 2$ to $F' = 2$ D_2 line of ^{87}Rb. The beam is elongated with two cylindrical lenses to cover the entire surface of the SLM along the x direction. A sinusoidal phase modulation along x is imprinted using a SLM and is limited to 0.1 radian so that the resulting intensity modulation does not locally modify the nonlinear index Δn. For a given k_x, the phase applied on the SLM is $\phi(x) = 0.1 \cos(k_x.x)$. In order to eliminate the unmodulated reflection on the SLM, we superpose a vertical grating to the horizontal sinusoidal one and select only the first vertical order in the Fourier plane. The SLM is imaged at the entrance of the nonlinear medium with a demagnification factor of 3, to increase its resolution. The beam waists at the medium entrance are $w_x = 0.15$ mm and $w_y = 1.5$ mm. We consider a local density approximation in order to compare the experimental data with the one-dimensional simulations. We verify that the fringe wavelengths are in agreement within 1% with the k_x imposed on the SLM.

As a nonlinear medium we used a 6.7 cm rubidium cell containing a natural mixture of 28% of ^{87}Rb and 72% of ^{85}Rb. The interaction parameter Δn is tuned by adjusting the cell temperature, hence the atomic density in the cell [32] and the laser detuning.

One should be careful that the linear absorption α increases when we tune the laser closer to resonance and

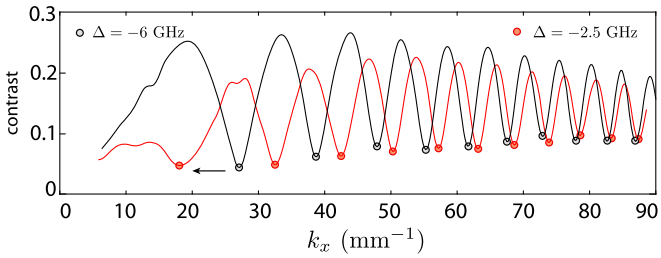

FIG. 3. Contrast for the off-resonance case (grey) with $\Delta n = 0$ and for a close-to-resonance set (red) with an input power of 90 mW, a cell temperature of 106 °C, and an absorption of 40%. For the weakly interacting case, the maximum contrast in the density standing wave is 0.25, which is within the Bogoliubov approximation. The shift of the minima of contrast toward the smaller k_x for the −2.5 GHz set, indicated by the black arrow, is evidence of the nonlinear effect taking place.

we maintain $\alpha \leq 13$ cm^{-1}. The output plane of the cell is then imaged on a camera. Typical beam images obtained for the noninteracting case ($\Delta n = 0$) are shown in Figs. 2(c) and 2(d) for $k_x = 27.8$ mm^{-1} (contrast minimum) and $k_x = 43.2$ mm^{-1} (contrast maximum). This noninteracting case is obtained experimentally by setting a large detuning ($\Delta = -6$ GHz) from the ^{87}Rb $F = 2$ to $F' = 2$ transition.

We then took 475 images of the cell output with modulations ranging from $k_x = 5$ mm^{-1} to $k_x = 100$ mm^{-1} with a step $dk_x = 0.2$ mm^{-1}. To measure the density modulation δn, we normalize the images by a reference taken without phase modulation and then select a central window of the fluid [see Fig. 2(e)]. After integration of the intensity along the y (vertical) axis, we calculate the contrast which is directly proportional to $\delta n(\tau = L/c)$. In Fig. 3, we plot the normalized contrast as a function of k_x and highlight the minima positions for a noninteracting ($\Delta = -6$ GHz) and a weakly interacting ($\Delta = -2.5$ GHz) fluid of light. For the latter case, we see a clear shift of the contrast minima toward smaller values of k_x, which indicates the presence of interactions.

We extract the structure factor from this contrast measurement using the methodology described previously. We first calibrate experimentally the phase imprinting efficiency of the SLM, the modulation transfer function of the optical system, and the depth of phase modulation by measuring the response function U for the noninteracting case. Since U is not modified while changing Δn, the structure factor for the interacting case is obtained by dividing the contrast maxima values for $\Delta n \neq 0$ by this calibrated value of U in order to obtain a normalization to 1 at large k_x. Experimentally, it corresponds to the ratio between the red and black maxima for the same p in Fig. 3. The results are presented in Fig. 4 for a weakly interacting fluid ($\Delta = -2.5$ GHz). The structure factor is a normalized, unitless quantity, that characterizes the spatial density-density correlations [19]. Figure 4 clearly shows that $S(k_x)$ is highly reduced at low k_x (long wavelength). This can be explained by the creation of correlated pairs at $+k_x$ and $-k_x$

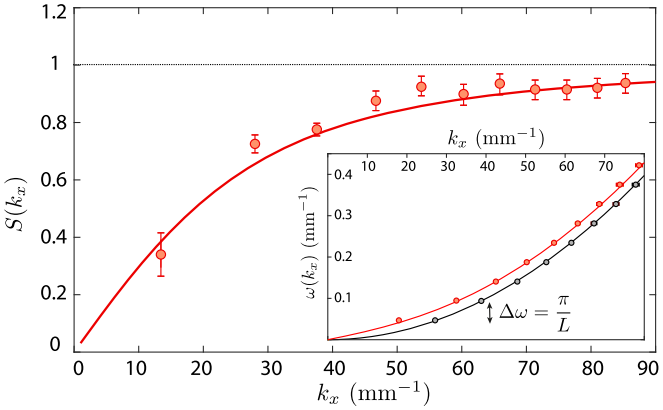

FIG. 4. Static structure factor measurement. The experimental conditions are the same as the red curve of Fig. 3. The dashed line at $S(k_x) = 1$ is the structure factor of a noninteracting gas (coherent state). The solid red line is the Feynman model given by Eq. (7) with the parameter $\Delta n = 4.6 \times 10^{-6}$ extracted from the measurement of the dispersion relation shown in the inset. Inset: dispersion relation for the noninteracting case (black) and for the weakly interacting case (red). Solid lines are fits using Eq. (3).

which minimize the total energy of the system, known as quantum depletion [18].

In our experimental configuration the number of points where this effect is highly visible (when $k_x < 1/\xi$) is limited by the cell length L. Indeed, if we require that the first contrast maximum occurs at $k_x = 1/\xi = k_0\sqrt{|\Delta n|}$, then the minimum cell length is given by $L = (2\pi/\sqrt{5}k_0|\Delta n|)$.

To complement our measurement of the structure factor, we provide a quantitative comparison with the Feynman relation [20,21,27]:

$$S(k_x) = \frac{k_x^2/2k_0}{\Omega_B(k_x)}. \tag{7}$$

The solid red line shown in Fig. 4 presents this relation with no adjustable parameters, since the dispersion relation $\Omega_B(k_x)$ at the denominator is measured independently as explained in the following.

To obtain the dispersion relation, we use the contrast measured as a function of k_x and record the successive minimum locations in k_x shown in Fig 3. Since, we have created two counterpropagating excitations in the fluid by imposing a phase modulation, minima occur when $\omega(k_x) = p(\pi/L)$, where p is an integer. In the inset of Fig. 4, we plot the dispersion relation (in red) by reporting the k_x positions of the contrast minima and assigning them a frequency $p\pi/L$. We compare it to the parabolic dispersion (in black) obtained with the same method in the noninteracting case by setting the fluid laser far-off resonance.

Fits using Eq. (3) are given in solid lines and they provide the value of Δn, which quantify the interactions. The dots are the experimental points and the full lines are

fits to the Bogoliubov relation. For the noninteracting case, we obtain the fit parameter $\Delta n = 0$ with an uncertainty of 2×10^{-7}. This value agrees, within the resolution of our experiment, with the expected quadratic dispersion $\omega_{\mathrm{lin}} = k_x^2/2k_0$ in the absence of interaction. For the interacting case, the fit of the Bogoliubov dispersion relation gives a value $\Delta n = 4.6 \times 10^{-6} \pm 3 \times 10^{-7}$. This is the value we used to plot the Feynman relation in order to compare it with our data without extra adjustable parameters in Fig. 4. Using the relation $c_s = c\sqrt{|\Delta n|}$, we can extract the sound velocity c_s from these fits [2,33] and we obtain $c_s = 2.1 \times 10^{-3} c$.

Finally, we evaluate the sensitivity of this method for resolving weak interaction (small $|\Delta n|$). The energy offset accumulated in the linear part of the dispersion translates into an energy shift at large k_x. The dispersion curve with $\Delta n \neq 0$ is vertically shifted relative to the noninteracting one ($\Delta n = 0$). We calculate this shift at large k_x as

$$\Omega_B(k_x) - \omega_{\mathrm{lin}}(k_x) = \sqrt{k_x^2|\Delta n| + \left(\frac{k_x^2}{2k_0}\right)^2} - \frac{k_x^2}{2k_0} \approx k_0|\Delta n|. \tag{8}$$

The value of Δn is then directly obtained by the difference with the noninteracting reference at high k_x. Knowing the uncertainty on k_x to be $dk_x = 0.2\ \mathrm{mm}^{-1}$, it is possible to estimate the smallest nonlinear index value achievable with this technique to be $\Delta n = 2 \times 10^{-7}$ ($c_s = 0.45 \times 10^{-3} c$). This is more than an order of magnitude better than previous techniques using a group velocity measurement [2].

Conclusion.—In this work, we present a measurement of the static structure factor in a paraxial fluid of light revealing a reduction of the small wave vector fluctuations, caused by the presence of pair-correlated particles. This measurement is based on an optical analogue of Bragg spectroscopy which has proved to be an essential tool to study ultracold atomic BECs and was missing in fluid of light platforms. Our results are robust to experimental noise and in quantitative agreement with the prediction of the Feynman relation, obtained by extracting the interaction strength from the experimental dispersion measurement. This work opens the way to the measurement of Tan's contact [34] and the observation of beyond mean field effects in photon fluids.

This work has received funding from the French ANR grants (C-FLigHT 138678 and "Quantum Fluids of Light" ANR-16-CE30-0021), from the European Union Horizon 2020 Research and Innovation Program under Grant Agreement No. 820392 (PhoQuS) and from the Region Île-de-France in the framework of DIM SIRTEQ. Q. G. and A. B. thank the Institut Universitaire de France (IUF). The authors thank Murad Abuzarli and Guillaume Brochier for additional numerical simulations and Antonine Rochet for support with 3D figures.

*quentin.glorieux@lkb.upmc.fr

[1] I. Carusotto, Superfluid light in bulk nonlinear media, Proc. R. Soc. A **470**, 20140320 (2014).
[2] Q. Fontaine, T. Bienaimé, S. Pigeon, E. Giacobino, A. Bramati, and Q. Glorieux, Observation of the Bogoliubov Dispersion in a Fluid of Light, Phys. Rev. Lett. **121**, 183604 (2018).
[3] C. Michel, O. Boughdad, M. Albert, P.-É. Larré, and M. Bellec, Superfluid motion and drag-force cancellation in a fluid of light, Nat. Commun. **9**, 2108 (2018).
[4] D. Vocke, K. Wilson, F. Marino, I. Carusotto, E. M. Wright, T. Roger, B. P. Anderson, P. Öhberg, and D. Faccio, Role of geometry in the superfluid flow of nonlocal photon fluids, Phys. Rev. A **94**, 013849 (2016).
[5] G. Situ and J. W. Fleischer, Dynamics of the Berezinskii–Kosterlitz–Thouless transition in a photon fluid, Nat. Photonics **14**, 517 (2020).
[6] P. Azam, A. Fusaro, Q. Fontaine, J. Garnier, A. Bramati, A. Picozzi, R. Kaiser, Q. Glorieux, and T. Bienaimé, Dissipation-enhanced collapse singularity of a nonlocal fluid of light in a hot atomic vapor, arXiv:2103.06637.
[7] M. Abuzarli, T. Bienaimé, E. Giacobino, A. Bramati, and Q. Glorieux, Blast waves in a paraxial fluid of light, Europhys. Lett. **134**, 24001 (2021).
[8] T. Bienaimé, M. Isoard, Q. Fontaine, A. Bramati, A. M. Kamchatnov, Q. Glorieux, and N. Pavloff, Quantitative Analysis of Shock Wave Dynamics in a Fluid of Light, Phys. Rev. Lett. **126**, 183901 (2021).
[9] N. Šantić, A. Fusaro, S. Salem, J. Garnier, A. Picozzi, and R. Kaiser, Nonequilibrium Precondensation of Classical Waves in Two Dimensions Propagating Through Atomic Vapors, Phys. Rev. Lett. **120**, 055301 (2018).
[10] K. E. Wilson, N. Westerberg, M. Valiente, C. W. Duncan, E. M. Wright, P. Öhberg, and D. Faccio, Observation of Photon Droplets and Their Dynamics, Phys. Rev. Lett. **121**, 133903 (2018).
[11] D. Vocke, C. Maitland, A. Prain, K. E. Wilson, F. Biancalana, E. M. Wright, F. Marino, and D. Faccio, Rotating black hole geometries in a two-dimensional photon superfluid, Optica **5**, 1099 (2018).
[12] M. Jacquet, T. Boulier, F. Claude, A. Maître, E. Cancellieri, C. Adrados, A. Amo, S. Pigeon, Q. Glorieux, A. Bramati *et al.*, Polariton fluids for analogue gravity physics, Phil. Trans. R. Soc. A **378**, 20190225 (2020).
[13] Y. Pomeau and S. Rica, Diffraction non linéaire, C. R.—Acadmie des Sciences **317**, 1287 (1993), http://sergiorica.com/Site/Publications_files/1993cCRAS317(diffr).pdf.
[14] T. Frisch, Y. Pomeau, and S. Rica, Transition to Dissipation in a Model of Superflow, Phys. Rev. Lett. **69**, 1644 (1992).
[15] Q. Fontaine, H. Hu, S. Pigeon, T. Bienaimé, E. Wu, E. Giacobino, A. Bramati, and Q. Glorieux, Attenuation-free non-diffracting Bessel beams, Opt. Express **27**, 30067 (2019).

[16] P. B. Blakie, R. J. Ballagh, and C. W. Gardiner, Theory of coherent Bragg spectroscopy of a trapped bose-einstein condensate, Phys. Rev. A **65**, 033602 (2002).
[17] J. Stenger, S. Inouye, A. P. Chikkatur, D. M. Stamper-Kurn, D. E. Pritchard, and W. Ketterle, Bragg Spectroscopy of a Bose-Einstein Condensate, Phys. Rev. Lett. **82**, 4569 (1999).
[18] D. M. Stamper-Kurn, A. P. Chikkatur, A. Görlitz, S. Inouye, S. Gupta, D. E. Pritchard, and W. Ketterle, Excitation of Phonons in a Bose-Einstein Condensate by Light Scattering, Phys. Rev. Lett. **83**, 2876 (1999).
[19] J. Steinhauer, R. Ozeri, N. Katz, and N. Davidson, Excitation Spectrum of a Bose-Einstein Condensate, Phys. Rev. Lett. **88**, 120407 (2002).
[20] P. Nozieres and D. Pines, *Theory of Quantum Liquids* (CRC Press, New York, 2018).
[21] A. Griffin, G. Allan *et al.*, *Excitations in a Bose-Condensed Liquid* (Cambridge University Press, Cambridge, England, 1993), Vol. 4.
[22] V. Kohnle, Y. Léger, M. Wouters, M. Richard, M. T. Portella-Oberli, and B. Deveaud-Plédran, From Single Particle to Superfluid Excitations in a Dissipative Polariton Gas, Phys. Rev. Lett. **106**, 255302 (2011).
[23] P. T. Ernst, S. Götze, J. S. Krauser, K. Pyka, D.-S. Lühmann, D. Pfannkuche, and K. Sengstock, Probing superfluids in optical lattices by momentum-resolved Bragg spectroscopy, Nat. Phys. **6**, 56 (2010).
[24] J. Steinhauer, N. Katz, R. Ozeri, N. Davidson, C. Tozzo, and F. Dalfovo, Bragg Spectroscopy of the Multibranch Bogoliubov Spectrum of Elongated Bose-Einstein Condensates, Phys. Rev. Lett. **90**, 060404 (2003).
[25] R. Ozeri, J. Steinhauer, N. Katz, and N. Davidson, Direct Observation of the Phonon Energy in a Bose-Einstein Condensate by Tomographic Imaging, Phys. Rev. Lett. **88**, 220401 (2002).
[26] I. Shammass, S. Rinott, A. Berkovitz, R. Schley, and J. Steinhauer, Phonon Dispersion Relation of an Atomic Bose-Einstein Condensate, Phys. Rev. Lett. **109**, 195301 (2012).
[27] R. P. Feynman, Atomic theory of the two-fluid model of liquid helium, Phys. Rev. **94**, 262 (1954).
[28] L. Pitaevskii and S. Stringari, *Bose-Einstein Condensation and Superfluidity* (Oxford University Press, New York, 2016), Vol. 164.
[29] Y. Zhang, J. Wen, S. N. Zhu, and M. Xiao, Nonlinear Talbot Effect, Phys. Rev. Lett. **104**, 183901 (2010).
[30] Y. Zhang, M. R. Belić, H. Zheng, H. Chen, C. Li, J. Song, and Y. Zhang, Nonlinear talbot effect of rogue waves, Phys. Rev. E **89**, 032902 (2014).
[31] J. Wen, Y. Zhang, and M. Xiao, The talbot effect: Recent advances in classical optics, nonlinear optics, and quantum optics, Adv. Opt. Photonics **5**, 83 (2013).
[32] C. B. Alcock, V. P. Itkin, and M. K. Horrigan, Vapour pressure equations for the metallic elements, Can. Metall. Q. **23**, 309 (1984).
[33] Q. Fontaine, P.-É. Larré, G. Lerario, T. Bienaimé, S. Pigeon, D. Faccio, I. Carusotto, É. Giacobino, A. Bramati, and Q. Glorieux, Interferences between Bogoliubov excitations in superfluids of light, Phys. Rev. Research **2**, 043297 (2020).
[34] S. Tan, Large momentum part of a strongly correlated Fermi gas, Ann. Phys. (Amsterdam) **323**, 2971 (2008).